Supporting Information

The Mechanism of Bending in a Plastically Flexible Crystal

Subhrajyoti Bhandary,[a] Amy J. Thompson,[b] John C. McMurtrie,[c,d] Jack K. Clegg,[b] Peuli Ghosh,[a] S. R. N. KiranMangalapalli,[e] Satoshi Takamizawa,[f] Deepak Chopra*[a]*

[a]*Department of Chemistry, Indian Institute of Science Education and Research Bhopal, Bhopal By-Pass Road, Bhopal, Madhya Pradesh, India-462066.*

[b]*School of Chemistry and Molecular Biosciences, The University of Queensland, St Lucia QLD 4072, Australia.*

[c]*School of Chemistry and Physics, Queensland University of Technology, 2 George Street, Brisbane QLD 4000, Australia.*

[d]*Centre for Materials Science,Queensland University of Technology, 2 George Street, Brisbane QLD 4000, Australia.*

[e]*Department of Physics and Nanotechnology, SRM Institute of Science and Technology, Kattankulathur, 603203, India*

[f]*Department of Materials System Science, Yokohama City University 22-2 Seto, Kanazawa-ku, Yokohama, Kanagawa 236-0027, Japan.*

E-mails: j.clegg@uq.edu.au, and dchopra@iiserb.ac.in

List of Contents

S1. Single Crystal Diffraction Study using Home Diffractometer andStructure Refinement

Single crystal X-ray diffraction (SCXRD) data of a straight single crystal (as grown) was collected on the Bruker D8 Venture (CMOS Photon 100) diffractometer using monochromated Mo Kα radiation (λ = 0.71073 Å). Data reduction was performed by Bruker Apex III software Suite[1]. The crystal structurewas solved by Intrinsic Phasing using the ShelXT program[2]. All structures were refined by the full-matrix least-squares method using ShelXL 2018 [3] present in the Olex2 interface[4]. All non-hydrogen atoms were refined anisotropically and all hydrogen atoms were positioned geometrically (hydrogen atom was located from the Fourier map when it is attached to nitrogen atom) and refined using a riding model.

Table S1. Crystal data and structure refinement parameters of **1**

Identification code	**1**
Empirical formula	$C_{16}H_9OF_4N$
CCDC	1989616
Formula weight	307.24
Temperature/K	100(2)
Crystal system	monoclinic
Space group	$P2_1/c$
a/Å	26.2128(8)
b/Å	5.00270(10)
c/Å	10.2514(3)
α/°	90
β/°	93.435(2)
γ/°	90
Volume/Å^3	1341.90(6)
Z	4
ρ_{calc}(g/cm^3)	1.521
μ/mm^{-1}	0.133
F(000)	624.0

Crystal size/mm^3	0.32 × 0.14 × 0.08
Radiation	MoKα (λ = 0.71073)
2Θ range for data collection/°	4.67 to 60.258
Index ranges	-31 ≤ h ≤ 36, -6 ≤ k ≤ 7, -14 ≤ l ≤ 14
Reflections collected	14917
Independent reflections	3929 [R_{int} = 0.0489, R_{sigma} = 0.0538]
Data/restraints/parameters	3929/0/202
Goodness-of-fit on F^2	1.045
Final R indexes [I>=2σ (I)]	R_1 = 0.0543, wR_2 = 0.1154
Final R indexes [all data]	R_1 = 0.0807, wR_2 = 0.1273
Largest diff. peak/hole / e Å^{-3}	0.35/-0.33

Table S2. List of important intermolecular interactions with geometrical parameters present in crystal of **1** [Cg1- C1 > C6, Cg2- C8 > C13].

motif	**Symmetry**	**D···A(Å)**	**H···A(Å)**	**D−H···A(^{0})**
N1-H1···O1	x, y+1, z	2.865(2)	1.88	160
Molecular Stacking		5.003(2)	-	-
Cg1···Cg1				
Cg2···Cg2				
C12-H12···F3	-x,-y,-z+1	3.859(2)	2.85	155
F2···F2		2.984(2)	-	-
F1···F2	-x, y-1/2, -z+1/2	2.915(2)	-	-
F3···F2		3.114(2)	-	-
C16(sp)···C16(sp)	-x+1,-y+1,-z+2	3.391 (3)	-	-
C16(sp)···C16(sp)	-x+1, y+1/2, -z+3/2	3.531(3)	-	-
C16(sp)-H16···C15(sp)		3.752(3)	2.81	145
C2-H2···C5	x, -y+1/2, z-1/2	3.963(2)	2.89	171
C2-H2···C16(sp)		4.022(2)	3.12	142
F4···C7		3.147(2)		
F4···C8		2.983(2)		

C5-H5···C2	x, -y-1/2, z-1/2	3.937(2)	2.87	172
C13-H13···C10		4.032(2)	3.02	156
C6-H6···C8		3.971(2)	3.03	146

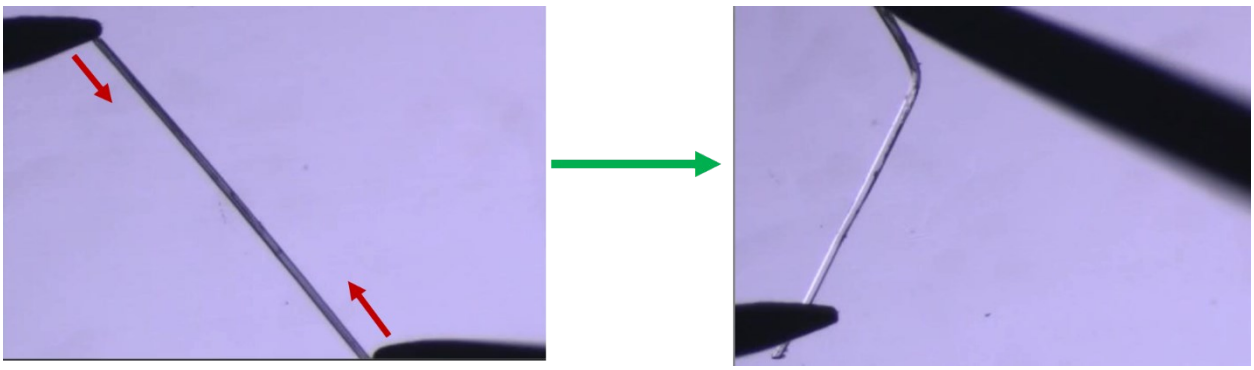

Figure S1. Bending of crystal **1** on (100) face by application of mechanical stress from two opposite faces (red arrows) of needle axis.

S2. Experimental Details of Measurements of Young's Modulus in Crystals (force measurement)

The force measurements were carried out on a Universal testing machine (Tensilon RTG-1210, A&D Co. Ltd.) at room temperature. A crystal specimen fixed on a glass base was pushed by a glass jig attached to a load cell. The Young's modulus (E) in each direction was obtained by fixing the end of the long side and pushing a narrow face (side surface, (001)) or a wide face (front surface, (100)) of the single crystal (see Figure 4a in the manuscript).

In this experiment, E is calculated using the following equation. $$E = \frac{W4d^3}{\delta\, bh^3}$$

W: weight, δ: displacement amount due to shearing, d: distance from a fixed position to a pressed position

b: the size of the crystal in the direction perpendicular to the shearing direction, h: crystal size in the direction along the shearing direction

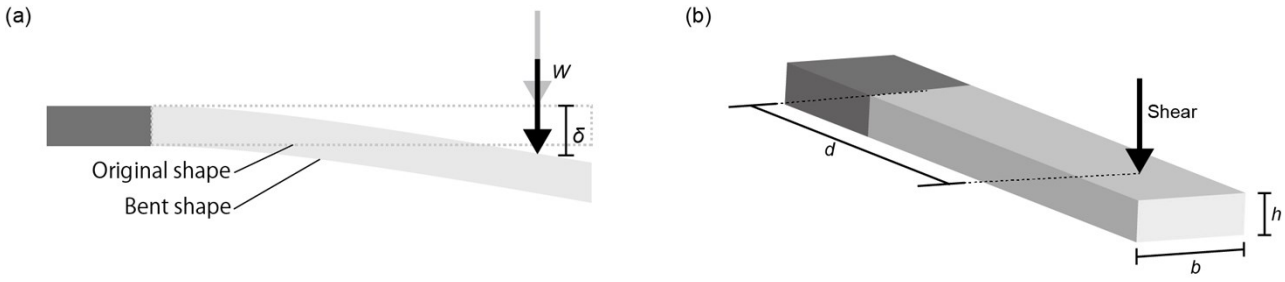

Figure S2. Illustration of the parameters used in the equation.

Among the parameters included in the equation, W / δ corresponds to the slope obtained by approximating the shear force vs. shear distance plot, obtained by force measurement by a straight line. Further, as shown in Figure S2, $4d^3/bh^3$ is a parameter related to the size of the crystal and is obtained from the microscope observation.

Figure S3 shows photographs ((i) to (v)) obtained when the crystal was sheared from the side. For the measurement, three different crystals are used, (i) to (iii) are the same crystal and (iv) and (v) are different crystals.

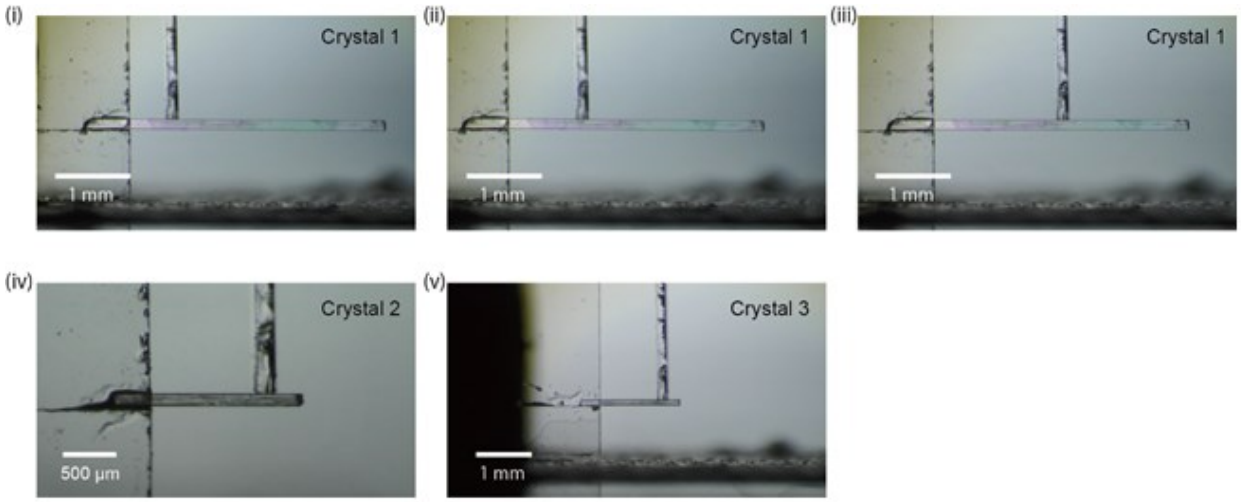

Figure S3. Photographs of crystal used for force measurement on (001) face.

The results of force measurement at this time is shown in the graph of Figure S4 below.

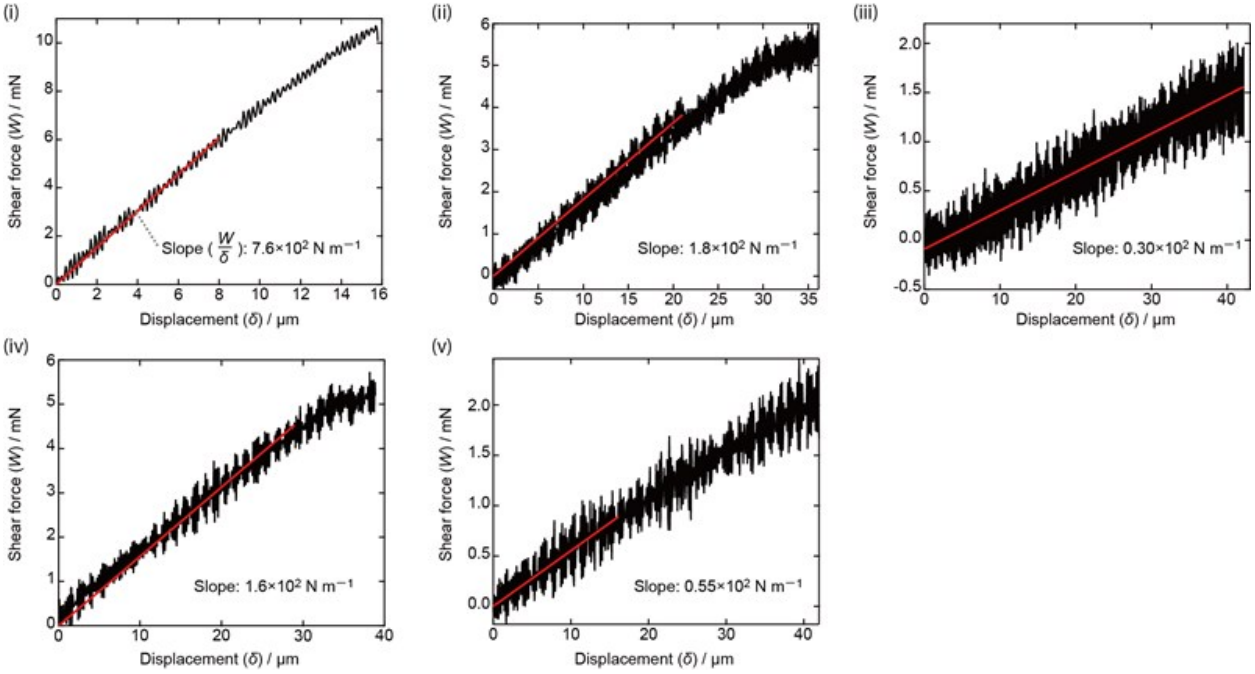

Figure S4. Results of force measurement on (001) face. The solid red line shows the fitting curve. A straight line passing through the origin was used for fitting.

Similarly, Figure S5 shows the photographs when shearing was performed from the front. Two different crystals were used for the measurement.

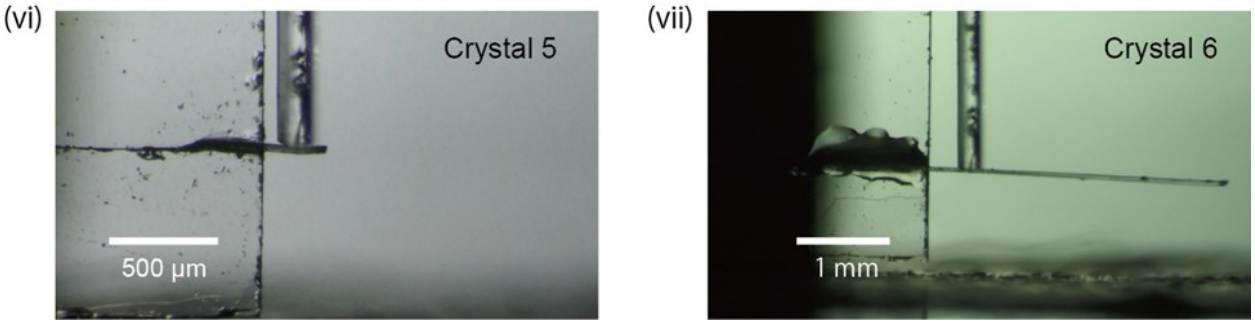

Figure S5. Photographs of crystals used for force measurement on (100) face.

The result of force measurement at this time is shown in the graph of Figure S6 below.

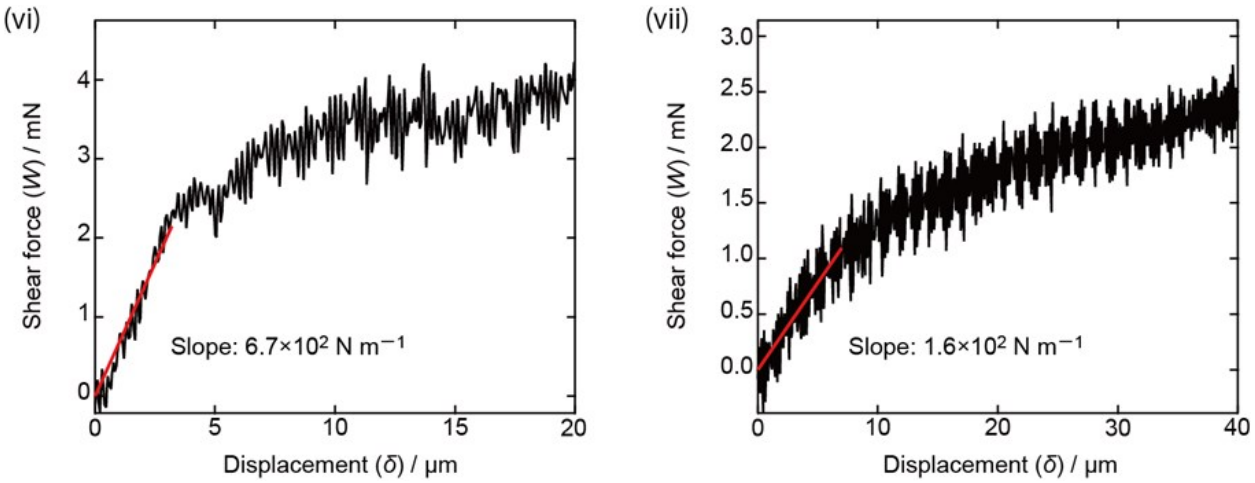

Figure S6. Result of force measurement on (100) face. The solid red line shows the fitting curve.

The E values calculated based on the above measurement is shown together with the parameters used in Table **S3**. In the measurement from the (001) face, the value was approximately 5 GPa (average value is 5.57 GPa). On the other hand, the measurement from the (100) face showed values of 0.1 to 0.2 GPa (average value is 0.135 GPa).

Table S3. Calculated Young's Modulus on different faces of the crystal

Face on		W/δ (Initial slope in Figs. S4, S6) (N m^{-1})	d (mm)	b (mm)	h (mm)	E (GPa)
Side (001)	(i)	7.6×10^2	0.573	0.0373	0.149	4.62
	(ii)	1.8×10^2	0.992			5.74
	(iii)	0.30×10^2	1.75			5.25
	(iv)	1.6×10^2	0.833	0.0525	0.101	6.69
	(v)	0.55×10^2	0.948	0.0345	0.0994	5.56
Front (100)	(vi)	6.7×10^2	0.150	0.0511	0.104	0.16
	(vii)	1.6×10^2	0.300	0.0456	0.152	0.11

S3. Nanoindentation Experiments

The nanoindentation experiments were performed on the (001) face of a bent crystal using a nanoindenter (Triboindenter of Hysitron, Minneapolis, USA). The machine continuously monitors and records the load (*P*) and displacement (*h*) of the indenter with force and displacement resolutions of 1 nN and 0.2 nm, respectively. A Berkovich diamond indenter (tip radius of ~100 nm) was used to indent the crystals. To identify flat regions for the experiment, the crystal surfaces were imaged before indentation using the same indenter tip. A loading and unloading rate of 0.6 mN/s and a hold time of 30 s at peak load were employed. The hardness and indentation modulus were calculated from the *P-h* curves using the Oliver-Pharr method. Ten indents were performed to get reliable and consistent data.

Table S4. H and E_{ind} measured from the nanoindentationtesting of the bent crystal at various positions on the (001) face.

Indent Position	**Hardness (H)**	**Indentation Modulus (E_{ind})**
1	74.50 ±5 MPa	0.65±0.12 GPa
2	111.95±22 MPa	1.75±0.37 GPa
3	228.24±8 MPa	2.22±0.21 GPa
4	330.3+15 MPa	3.97±0.45 GPa

S4. Micro-focused SCXRD Mapping Experiments using Synchrotron Radiation

Micro-focus SCXRD for the mapping experiment was performed at the Australian Synchrotron MX2 beamline[5]. All of the measurements were performed at 100(2) K using the wavelength λ = 0.7108 Å. A full data collection was performed with a beam cross-section (full-width at half-maximum (FWHM)) of 22 x 12 μm. Mapping studies were performed using a microcollimator that produced a beam cross-section of 7.5 x 11.25 μm (FWHM). Data acquisition was performed using AS QEGUI[6]. Data was collected in 20° wedges to minimize interference from the shoulders of the crystal, moving 2 μm between collections. Data integration and reduction was performed using the XDS package[7]. The unbent structure (collected as a full 360° scan) was solved with ShelXT[2] and

refined with ShelXL[3] using the Olex2 graphical interface[4]. Data from the mapping experiments were refined against the reference solution using ShelXL[3]. Rigid body restraints were applied to assist refinement with the necessary low completeness. Consequently, all structures were refined isotropically to maintain reasonable data to parameter ratios. Full CIF files are supplied. The isotropic refinement and a limited number of diffraction images collected for the mapping studies results in a number of CheckCIF Level A and B alerts. CCDC numbers 1981921-1981933.

Mapping Experiment:

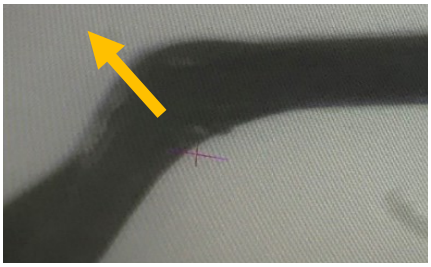

Figure S7. Image of the first bent crystal. Mapping was undertaken along the yellow arrow. Due to the off-set angle, there is some uncertainty in the exact distance covered, so the analysis is presented relative to position numbers.

The distribution of cell parameters across the various points of the bent crystal are given in Figure S8. A horizontal line was fitted to the mean of each parameter, with the 95% confidence intervals given in Table S5. The errors in the cell parameters obtained from data integration and refinement are also presented in Table S5. While the axes are slightly elongated compared to the unit cell of the unbent crystal, this is due to higher mosaic spread. Additionally, no significant changes are observed across the crystal, and the errors in the cell axes are often considered to be underestimated. To further analyze if the cell parameters were statistically constant, 95% prediction intervals were calculated based on the mean. As Figure S8 shows, the majority of the data points lie within this region. Therefore, the conclusion that the cell parameters are not significantly changing remains valid. The apparent randomness in the data is a result of the explained experimental errors. Three data sets in the middle were removed as they did not provide satisfactory refinements. This is likely due to increased dislocations measured as the centre position would contain more compared to the edges.

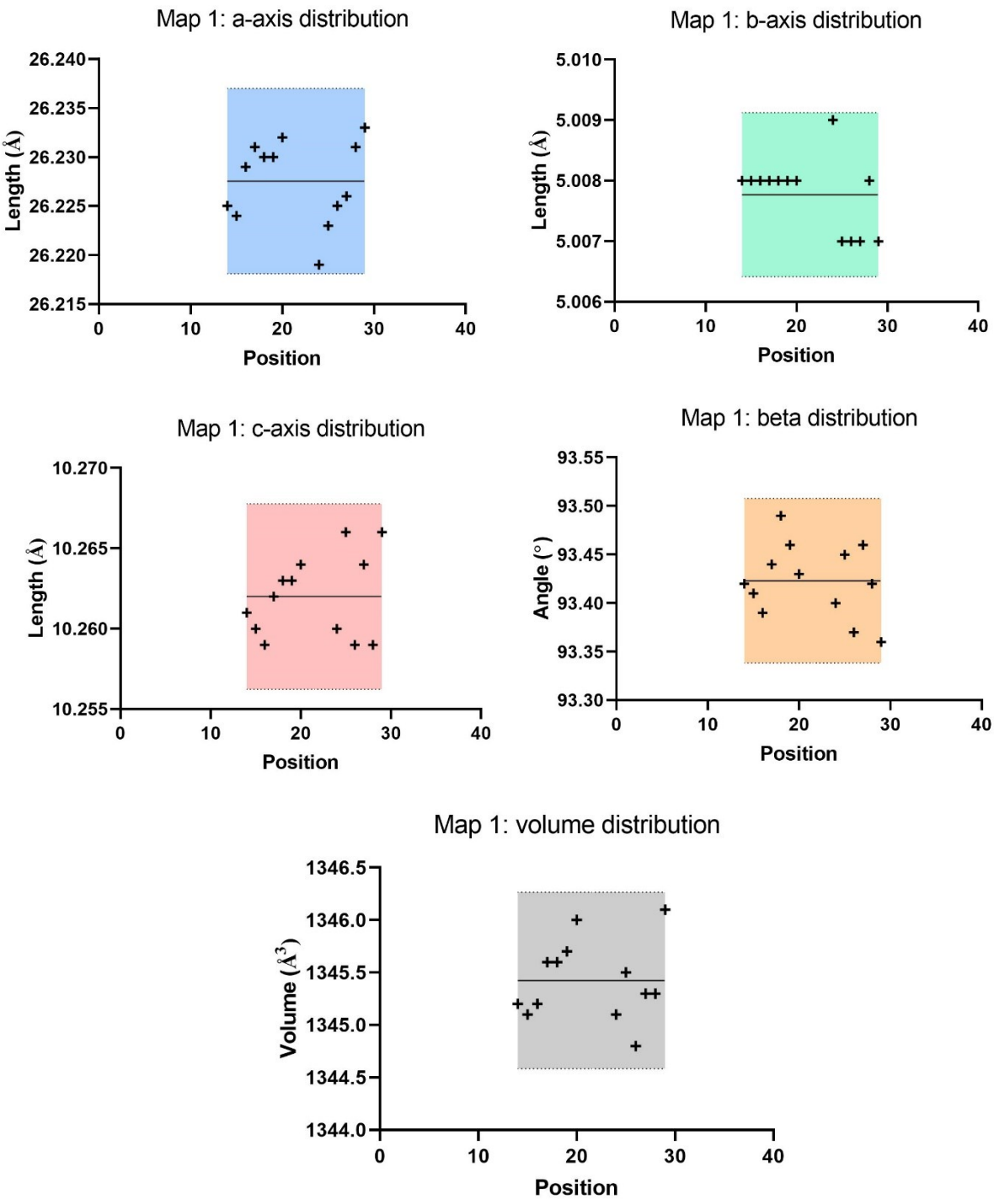

Figure S8. Graphs of the variation in cell parameters over distance for Map 1. Note the shaded area which represents the 95% prediction interval for the calculated horizontal line of best fit.

Table S5: Statistics of the horizontal linear fit to Map 1

Parameter	*a*-axis (Å)	*b*-axis (Å)	*c*-axis (Å)	β (°)	Volume (Å^3)
Mean	26.23	5.008	10.26	93.42	1345
95% CI	26.23-26.23	5.007-5.008	10.26-10.26	93.40-93.45	1345-1346
Standard Deviation	0.004	0.001	0.003	0.04	0.4
Error in mapping cell parameter (from CIFs)	0.005	0.001	0.002	0.03	0.5

S5. Calculations on Energy frameworks

Energy frameworks for crystal **1** have been constructed from pairwise intermolecular interaction energy calculations (at crystal geometry) using the CE-B3LYP/ 6-31g (d, p) molecular wave functions in *CrystalExplorer17.5*.[8] Total interaction energy has been partitioned into electrostatic, polarization, dispersion and exchange-repulsion terms can be obtained from a *scaling scheme*.[9] Frameworks were shown at energy cut off of -5 kJ/mol and tube size of 80.

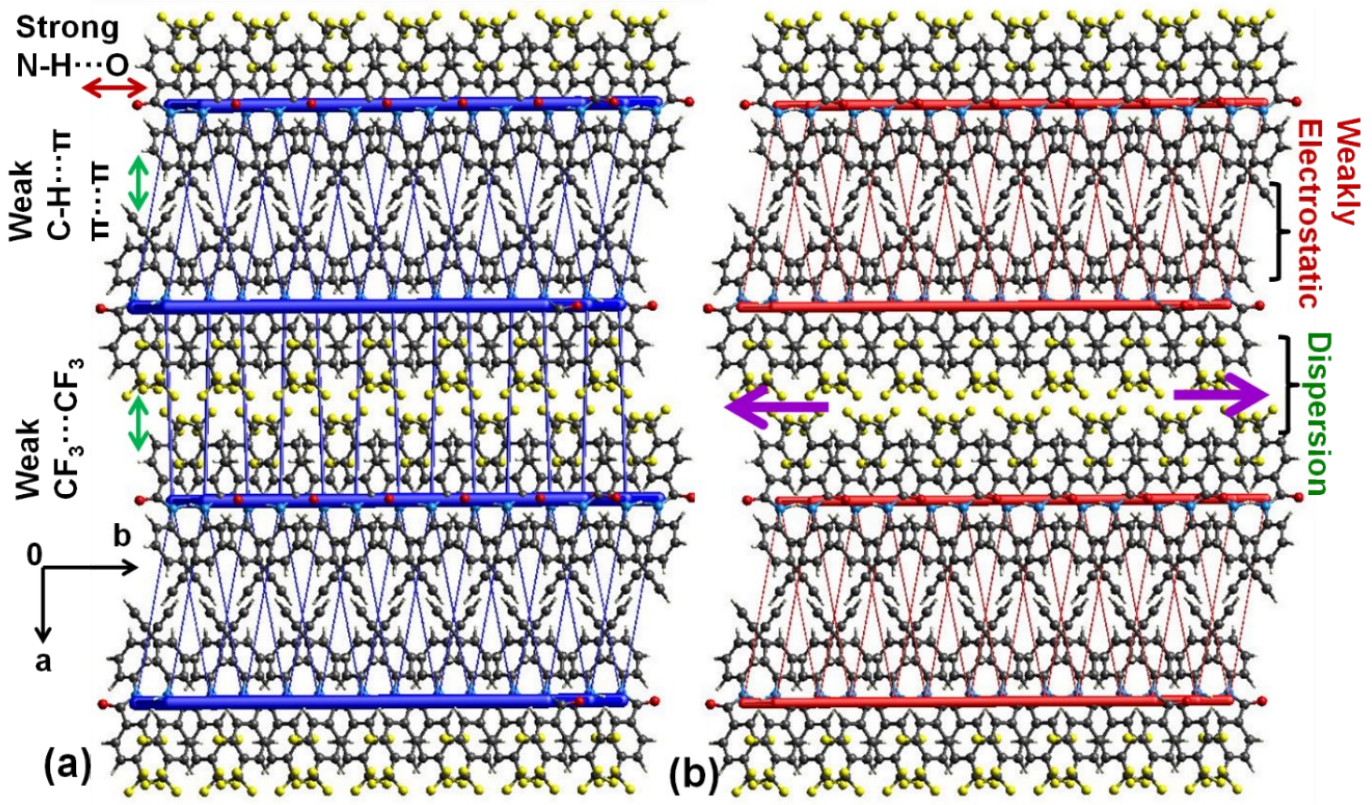

Figure S12. Interaction topology of molecules in terms of (a) total energy framework and (b) decomposed electrostatic framework, revealing energetic rationalization for ultra-plastic flexibility and shape-shifting effect in the single crystal of **1**. Double headed arrows depict the direction of important intermolecular interactions. Purple arrows indicate directions of layer sliding.

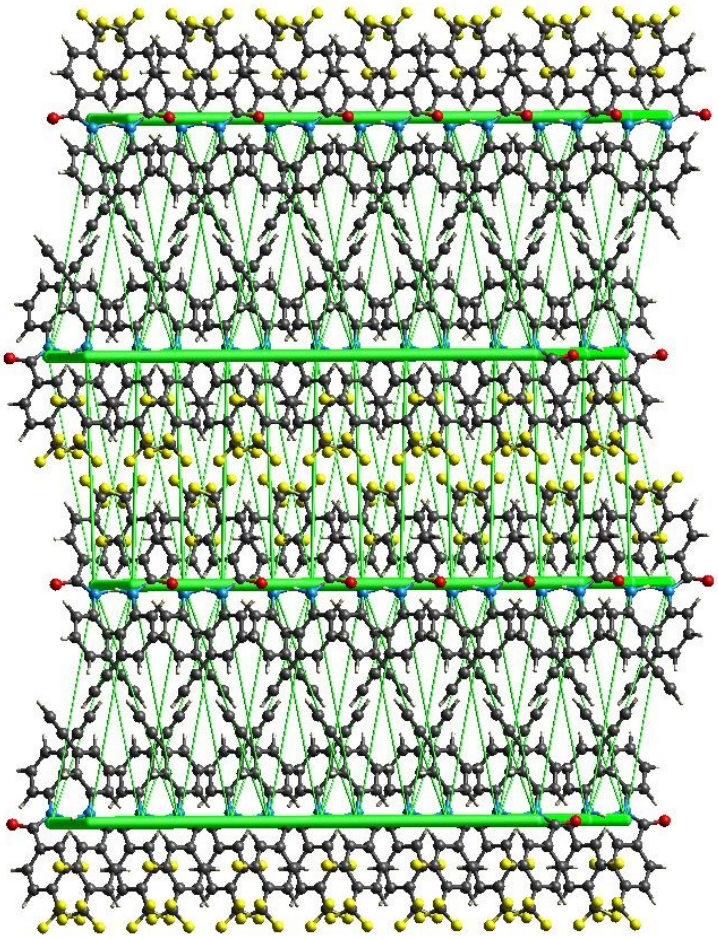

Figure S13. Dispersion component of energy framework for **1** computed at the same crystallographic direction as Figure S12.

Output of energy framework calculations for 1 crystal:

1

Interaction Energies (kJ/mol)
R is the distance between molecular centroids (mean atomic position) in Å.

Total energies, only reported for two benchmarked energy models, are the sum of the four energy components, scaled appropriately (see the scale factor table below)

	N	Symop	R	Electron Density	E_ele	E_pol	E_dis	E_rep	E_tot
	0	-x, y+1/2, -	13.51	B3LYP/6-31G(d,p)	0.7	-0.1	-6.6	1.5	-4.2

		z+1/2							
	0	-x, -y, -z	11.43	B3LYP/6-31G(d,p)	-4.0	-0.4	-13.8	4.3	-13.9
	0	-x, -y, -z	12.25	B3LYP/6-31G(d,p)	-0.4	-0.1	-2.5	0.1	-2.6
	1	x, y, z	5.00	B3LYP/6-31G(d,p)	-40.0	-10.2	-49.6	56.7	-57.9
	0	x, -y+1/2, z+1/2	5.96	B3LYP/6-31G(d,p)	-6.6	-1.9	-37.3	20.4	-28.2
	2	-x, y+1/2, -z+1/2	15.21	B3LYP/6-31G(d,p)	-4.9	-0.8	-6.5	8.4	-6.2
	1	-x, -y, -z	16.38	B3LYP/6-31G(d,p)	-0.7	-0.2	-5.1	1.0	-4.7
	2	x, -y+1/2, z+1/2	5.49	B3LYP/6-31G(d,p)	-5.5	-2.2	-35.5	18.0	-27.1
	1	-x, -y, -z	16.97	B3LYP/6-31G(d,p)	0.4	-0.5	-7.2	6.0	-2.5

Scale factors for benchmarked energy models
See Mackenzie et al. IUCrJ (2017)

Energy Model	k_ele	k_pol	k_disp	k_rep
CE-HF ... HF/3-21G electron densities	1.019	0.651	0.901	0.811
CE-B3LYP ... B3LYP/6-31G(d,p) electron densities	1.057	0.740	0.871	0.618

S6. References

1. Bruker, Apex3, M86-E01078, Bruker Analytical X-ray Systems Madison, WI, **2016**.
2. Sheldrick, G. M. *Acta Crystallogr A Found Adv.* **2015,** *71* (Pt 1), 3-8.
3. Sheldrick, G. M. *Acta Crystallogr C Struct Chem.***2015,** *71* (Pt 1), 3-8.
4. Dolomanov,O. V.;Bourhis,L. J.;Gildea,R. J.; Howard,J. A. K.; Puschmann,H.*J. Appl. Crystallogr.* **2009,***42* (2), 339-341.
5. Aragao, D.; Aishima, J.; Cherukuvada,H.;Clarken,R.; Clift,M.; Cowieson,N. P.; Ericsson,D. J.;Gee,C. L.; Macedo,S.;Mudie,N.;Panjikar,S.; Price, J. R.; Riboldi Tunnicliffe, A.; Rostan, R.; Williamson,R.;Caradoc-Davies,T. T. *J. Synchrotron Radiat* **2018,** *25* (Pt 3), 885-891.
6. Ryder,A.; Jackson, G.;Owen,A.;Fernandes,R.;Maksimenko,A.;Pozar,A.;Starritt,A.*AS QEGui*,https://qtepics.github.io/, 2019.
7. Kabsch, W.*J. Appl. Cryst.* **1993,** *26*, 795-800.
8. Turner, M. J.; McKinnon, J. J.; Wolff, S. K.; Grimwood, D. J.; Spackman, P. R.; Jayatilaka, D.; Spackman, M. A. *CrystalExplorer17*, **2017**. University of Western Australia. http://hirshfeldsurface.net
9. Mackenzie, C. F.; Spackman, P. R.; Jayatilaka, D.; Spackman, M. A. *IUCrJ* **2017**, *4*, 575.